Shape measurement using one frame projected sawtooth fringe pattern

Chen, Lujie; Quan, Chenggen; Tay, Cho Jui; Fu, Yu

2005

Chen, L., Quan, C., Tay, C. J., & Fu, Y. (2005). Shape measurement using one frame projected sawtooth fringe pattern. Optics Communications, 246(4-6), 275-284.

https://hdl.handle.net/10356/91209

https://doi.org/10.1016/j.optcom.2004.10.079

Shape measurement using one frame projected sawtooth fringe pattern

Lujie Chen *, Chenggen Quan, Cho Jui Tay, Yu Fu

Department of Mechanical Engineering, National University of Singapore, 10 Kent Ridge Crescent, Singapore 119260, Singapore

* Corresponding author. Tel./fax: + 65 687 422 30.
E-mail address: g0202094@nus.edu.sg (L. Chen).

Abstract

Fringe projection technique is a non-contact, full field shape measurement method. The object depth information is recorded as sinusoidal or square wave fringe patterns. The phase-shifting technique or Fourier transform method can be used to extract wrapped phase data and a continuous phase distribution can be retrieved by a phase unwrapping process. In this paper, a shape measurement method using one frame projected sawtooth fringe pattern is proposed. A computer-generated sawtooth pattern is projected by a programmable liquid crystal display (LCD) projector. The deformed sawtooth pattern encoding object shape is converted to a wrapped phase map without using phase shifting or Fourier transform and a continuous phase distribution is retrieved by a quality-guided phase unwrapping algorithm. A special phase quality map, capable of detecting invalid shadowed phase data, is proposed to facilitate the unwrapping process.

Keywords: Phase retrieval; Fringe projection; Sawtooth fringe pattern; Phase unwrapping

1. Introduction

Optical techniques for 3D shape measurements have been widely studied [1], as the conventional approach using mechanical probes is not suitable for non-contact or full field measurement. Numerous methods, such as those based on the moiré, interferometry and fringe projection technique, have been developed.

In moiré technique [2,3], an object profile is coded into a moiré fringe pattern produced by one (shadow moiré) or two (projection moiré) gratings. The phase angle of the fringe pattern is related to the object surface depth and can be extracted by well-known fringe analysis algorithms, such as phase-shifting and Fourier transform methods. The moiré technique is useful for measuring small objects but its application for large

object measurement is limited by the size of the gratings and the measurement accuracy is dependent on the resolution of the gratings.

Shape measurement techniques based on interferometry, such as those using the Newton, Fizeau and Michelson interferometers, have been known for a long time [4]. Although the basic set-ups of these interferometers are simple, they can be developed into various forms depending on applications [5,6]. The advantage of interferometry based techniques is that high measurement accuracy, a fraction of the wave length of light, can be achieved. However, the surface of the test object must be highly reflective and monochromatic light source must be used for interference. In recent years, another trend in 3D shape or surface roughness measurement is based on white light (incoherent light) interferometry [7,8]. The accuracy of the techniques using white light is even higher than that using coherent light because the coherent length of white light is very short and the generation of white light fringe pattern ensures high accuracy. However, since white light fringe pattern is observable only in a small range, it is necessary to scan perpendicularly though an object surface to reconstruct a 3D profile. Hence, the measurement speed is relatively slow and large amount of data is involved in processing.

Fringe projection technique is based on the principle of triangulation [9]. Before the advent of digital fringe projector, gratings served as the source of fringe pattern. The most commonly used is a square wave grating, which is composed of transparent and dark stripes. Takeda and Mutoh [10] proposed a carrier fringe Fourier transform method to extract phase data from a square wave fringe pattern. Srinivasan et al. [11] applied phase-shifting algorithm to extract an object surface profile from a projected sinusoidal grating. Similar to moiré technique, the accuracy of both methods is dependent on the resolution of the gratings. The advent of the digital fringe projector, such as the programmable liquid crystal display (LCD) projector, has advanced the fringe projection technique. Any computer-generated fringe pattern can be projected. Furthermore, phase shifting, fringe density and intensity can be changed digitally without modifying the physical set-up. A number of papers have reported the use of the digital projection device. Coggrave and Huntley [12] studied the precision of a shape measurement system based on a LCD projector. Sansoni et al. [13] developed a gray-code light projection technique, which could be used to evaluate objects with discontinuous surface. Quan et al. [14] applied the LCD projector on small object measurement. Huang et al. [15] used a color projector to introduce phase shifts into the red, green and blue (RGB) components of a color fringe pattern and a three-step phase-shifting algorithm is applied to the subsequently separated RGB components. Fang and Zheng [16] proposed a linearly coded profilometry technique, in which an isosceles or a right-angle triangle sawtooth pattern is projected to encode an object profile. They developed a sawtooth-pattern-oriented phase-shifting algorithm and at least three frames are needed for the isosceles triangle pattern and two frames for the right-angle triangle pattern.

In this paper, a shape measurement method using only one frame (right-angle triangle) sawtooth pattern is presented. A wrapped phase map is obtained through a linear translation of the recorded sawtooth pattern, instead of using the phase-shifting or Fourier transform method. A quality-guided phase unwrapping algorithm [17] is used to retrieve the unwrapped phase map. However, since the wrapped phase map is ob-

tained in an unconventional way, current phase quality criteria [17,18] are not able to detect shadow areas. A recent paper has shown that based on least-square sinusoidal fitting a good phase quality map can be generated [19]. Similar technique is implemented in this paper and the effectiveness of the new technique is compared with the phase derivative variance quality criterion.

2. Principle of the method

2.1. Wrapped phase map extraction

Different measurement set-ups can be used to encode an object profile and Fig. 1 shows a typical arrangement of the projection and imaging system. Point P and E are the centers of the exit pupil for the projection and imaging optics, respectively. If the object size is small compared to the distance from the object to the image plane and under normal viewing conditions, the surface height $h(x,y)$ can be expressed in terms of L (the distance between the point E and the reference plane), D (the horizontal distance between point P and E) and $\overline{BC}$ by applying the similarity between triangle ABC and APE, as shown in Fig. 1 [9–11]:

$$h(x,y) = \frac{L \cdot \overline{BC}}{D + \overline{BC}}, \tag{1}$$

where $\overline{BC}$ is proportional to the phase angle $\phi(x,y)$ to be measured. As $\overline{BC}$ is relatively small compared to D, Eq. (1) can be simplified as

$$h(x,y) = \frac{L \cdot c}{D}\phi(x,y), \tag{2}$$

where c is a constant coefficient that relates $\overline{BC}$ with $\phi(x,y)$ and is determined by parameters such as illuminating and capturing angle, and pitch of the fringe pattern. Generally, the term $L \cdot c/D$ in Eq. (2) is considered as a calibration coefficient, which can be obtained experimentally from the ratio of a known displacement to the calculated phase difference [14].

To encode an object surface profile, a sawtooth pattern is generated for projection. The solid points in Fig. 2(a) represent the intensity of a cross-section of the computer-generated sawtooth pattern, which can be expressed as

$$I(x,y) = a + b \cdot W[2\pi fx + \phi(x,y)], \tag{3}$$

where a and b are constant background and modulation intensity, respectively; W[...] represents an operator that wraps a phase angle into $[-\pi, \pi]$, f is the spatial fringe frequency, and $\phi(x,y)$ is related to the surface height. Since a and b are uniform theoretically, the intensity $I(x,y)$ is

linearly related to the wrapped phase angle $\phi_w(x,y) = 2\pi f x + \phi(x,y)$. Hence, a translation function can be used to extract the wrapped phase angle:

$$\phi_w(x,y) = \alpha \cdot I(x,y) + \beta, \tag{4}$$

where α and β are translating parameters retrievable from the global maximum ($I_{\max}$) and minimum ($I_{\min}$) intensities of the sawtooth pattern.

$$\begin{cases} \alpha \cdot I_{\max} + \beta = \pi, \\ \alpha \cdot I_{\min} + \beta = -\pi, \end{cases} \Rightarrow \begin{cases} \alpha = \frac{2\pi}{I_{\max} - I_{\min}}, \\ \beta = -\pi \cdot \frac{I_{\max} + I_{\min}}{I_{\max} - I_{\min}} \end{cases} \tag{5}$$

When α and β are determined, the intensity of each pixel is fed into Eq. (4) to calculate the corresponding wrapped phase value. The resultant phase map after phase unwrapping contains a linear component $2\pi f x$, which must be subtracted. The spatial frequency f can be found using Fourier transform method [10] in frequency domain or by directly detecting the slope of the unwrapped phase map in spatial domain.

The above proposed is the basic idea of intensity to phase conversion. However, when the computer-generated sawtooth pattern is projected and imaged, the intensity distribution recorded would not be perfectly uniform. The hollow points in Fig. 2(a) shows a simulated intensity cross-section recorded on a CCD camera. There are several intermediate pixels between a peak and valley due to defocus, which has a spatially average effect. Since the recorded intensity of a pixel (hollow point) is the average intensity of a small region on an object surface, which in turn is the average intensity of a few pixels on the LCD panel, severe distortion would occur at a local region containing a peak and valley. The sharpness of a sawtooth pattern is reduced and the intermediate pixels do not encode the surface profile. If such intensity pattern is converted into a wrapped phase map, there would not be 2π phase jumps for phase unwrapping. Fang [16] proposed to overcome the problem by using multiple samples such as fringe patterns with different pitches. In this study, however, an image processing algorithm is proposed to reset the intensity of intermediate pixels. The program scans each cross-section perpendicular to the fringes, identifying all pairs of peak and valley. An intermediate pixels ' intensity is then reset based on the slope of a data line, since the slope preserves the trend of intensity variation which reflects the trend of shape change. For example, in Fig. 2(a) an intermediate pixel indicated by an arrow is closer to a peak. Its modified intensity is given by:

$$I_{\mathrm{m}} = I_{\mathrm{p}} + s \cdot d, \tag{6}$$

where I_{p} is the intensity of the nearby peak; s is the slope calculated using several data points ahead of the peak; d represents the distance between the peak and the intermediate pixel under consideration. For an intermediate pixel closer to a valley, its modified intensity can be obtained in a similar way. Fig. 2(b) shows the intensity distribution after

processing. As can be seen, the sharpness of the sawtooth pattern is recovered and the arrow indicates the modified intensity of the pixel under consideration. Although theoretically the slope-based intensity modification does not retrieve the actual height information from intermediate pixels, it can effectively compensate phase measurement errors and facilitates subsequent phase unwrapping process by recovering the data jumps between two fringe periods.

Non-uniform illumination and reflectance also reduce the uniformity of the recorded intensity distribution, which is more appropriate to be expressed in terms of varying rather than constant background and modulation intensities.

$$I'(x,y) = a(x,y) + b(x,y)\phi_w(x,y), \tag{7}$$

where $a(x,y)$ and $b(x,y)$ undergo low-frequency variations in comparison to $\phi(x,y)$ as long as the illumination and reflectance do not change drastically. The intensity cross-section in Fig. 2(b) shows higher background at the center and smaller modulation at the right side. Under this circumstance, if the global maximum and minimum intensities are used to determine the translating parameters α and β, large amount of error would be produced in phase conversion because $I'(x,y)$ is not globally linear to $\phi_w(x,y)$ with varying $a(x,y)$ and $b(x,y)$. However, within one sawtooth fringe period at an arbitrary cross-section, $I'(x,y)$ can be considered linear to $\phi_w(x,y)$ based on the assumption that $a(x,y)$ and $b(x,y)$ are slow-varying compared to $\phi_w(x,y)$. Hence, a pair of α and β associated with each cross-sectional fringe period is obtained from the local maximum and minimum intensities, and is subsequently used to convert the intensities of the corresponding fringe period to phase angles. Fig. 2(c) shows the wrapped phases obtained. The previously non-uniform background and modulation (Fig. 2(b)) is unified.

2.2. Quality map for quality-guided phase unwrapping algorithm

Fig. 3 shows a sawtooth pattern projected on a fish model and Fig. 4 is the extracted wrapped phase map. A quality-guided phase unwrapping algorithm [17] is used to unwrap the phase map. The key factor of the algorithm is to find a quality map to facilitate the unwrapping process. Figs. 5(a) and (b) show, respectively, 3D plot of a high quality region *ABCD* and low quality region *EFGH*, as indicated in Fig. 4. The data planes are uniform with a high degree of planity in the former but less planity in the later, indicating that the phase quality is related to the degree of planity. Furthermore, in consideration that shadow areas at the fin and tail of the fish model (Fig. 4) contain flat data planes with good planity, the slope of a plane should also be incorporated into the quality criterion to distinguish valid data having a slope that follows the linear phase component (Eq. (3)) from shadowed phases with nearly zero slopes. A least-square plane-fitting scheme is proposed to generate the quality criterion, since the fitting error reflects the degree of planity and the normal vector of the fitted plane contains the slope information. The quality criterion for a pixel under consideration is developed by evaluating $N \times N$ neighboring pixels. A plane in 3D Cartesian coordinate is expressed as

$$z = k_x \cdot x + k_y \cdot y + z_0, \tag{8}$$

where (x,y) locates a pixel in the phase map, z represents the phase value, $(-k_x, -k_y, 1)$ is the normal vector of the plane, and z_0 is the intersection of the plane and z axis. To fit the plane to the phase data, an error parameter defined by:

$$E(x,y) = \sum_{i=x-\frac{N}{2}}^{x+\frac{N}{2}} \sum_{j=y-\frac{N}{2}}^{y+\frac{N}{2}} \left[\phi_w(i,j) - (k_x \cdot i + k_y \cdot j + z_0)\right]^2 \tag{9}$$

is used. The parameter is minimized and the partial derivatives of $E(x,y)$ with respect to k_x, k_y and z_0 are set to zero

$$\begin{cases} \frac{\partial E(x,y)}{\partial k_x} = -2 \cdot \sum_{i=x-\frac{N}{2}}^{x+\frac{N}{2}} \sum_{j=y-\frac{N}{2}}^{y+\frac{N}{2}} \\ \qquad \times \left[\phi_w(i,j) - (k_x \cdot i + k_y \cdot j + z_0)\right] \cdot i = 0, \\ \frac{\partial E(x,y)}{\partial k_y} = -2 \cdot \sum_{i=x-\frac{N}{2}}^{x+\frac{N}{2}} \sum_{j=y-\frac{N}{2}}^{y+\frac{N}{2}} \\ \qquad \times \left[\phi_w(i,j) - (k_x \cdot i + k_y \cdot j + z_0)\right] \cdot j = 0, \\ \frac{\partial E(x,y)}{\partial z_0} = -2 \cdot \sum_{i=x-\frac{N}{2}}^{x+\frac{N}{2}} \sum_{j=y-\frac{N}{2}}^{y+\frac{N}{2}} \\ \qquad \times \left[\phi_w(i,j) - (k_x \cdot i + k_y \cdot j + z_0)\right] = 0. \end{cases} \tag{10}$$

The values of k_x, k_y and z_0 are obtained using Eq. (10) and on substituting these values into Eq. (9) the fitting error $E(x,y)$ is obtained.

The criterion for the phase quality is defined as [19]

$$R(x,y) = \frac{K_{x,y}}{c_1 + \frac{E(x,y)}{K_{x,y}}}, \tag{11}$$

$$K_{x,y} = \frac{|k_x|}{c_2 + |k_y|}, \tag{12}$$

where c_1 and c_2 are variable coefficients used to prevent the denominator from being zero. The parameter $K_{x,y}$ relates to the slope of the fitted plane. Based on the linear phase component $2\pi fx$ in Eq. (3), $|k_x|$ should be large and $|k_y|$ should be zero. In a shadowed or noisy area either small $|k_x|$ or large $|k_y|$ would be found, which results in a small value of $K_{x,y}$. The fitting error $E(x,y)$ ensures that the larger the error, the less is the planity and

thereby lower phase quality.

A remaining technical problem in phase quality identification is that a 2π phase jump between each fringe period would produce errors in plane-fitting. Therefore, it is necessary to apply a primitive unwrapping process, such as raster unwrapping [17], to remove most of the 2π phase jumps in a processing window prior to plane-fitting.

3. Experimental work

The surface profile of a fish model ($40 \times 30\text{mm}^2$) is studied. A computer-generated sawtooth fringe pattern is loaded into the LCD projector though a controller, as shown in Fig. 1. A camera lens mounted on the exit pupil of the LCD projector is used to focus the projected sawtooth pattern on the object surface. The sawtooth pattern is recorded using a CCD camera and the video signal is stored in a computer for further processing. The sensitivity of the system increases with the projection angle. However, a large angle would produce shadows on the object surface, which reduce fringe information and hinders the retrieval of a continuous phase distribution. In the experiment, the projection angle is set at 25°, however, there are still some shadow areas due to the drastic surface profile changes (Fig. 3). A phase quality criterion minimizing shadow effect is discussed in the next section.

The nonlinearity of the system which would have a significant effect on the experimental results is also studied. The LCD projector provides a resolution of 832×624 pixels, each can assume a gray value of between 0 and 255. The CCD camera has a resolution of 768×576 pixels with 256 intensity levels. The apertures of the camera lens on the LCD projector and the CCD camera are first set at a suitable value and 18 computer-generated images, each with a constant intensity, are projected on a reference plate. The mean intensity of each image recorded by the CCD camera against the input computer-generated intensity is studied. It is found that the system nonlinearity is most severe when the input intensity level is above 230 and below 30. Hence, the maximum and minimum intensity levels of a computer-generated sawtooth pattern are set at 230 and 30, respectively.

4. Results and discussion

4.1. Conversion of sawtooth fringe pattern to wrapped phase map

Fig. 6(a) shows the intensity of cross-section A– A as indicated in Fig. 3. As can be seen, there are several intermediate pixels between an adjacent peak and valley. Fig. 6(b) shows the intensity distribution after the intensity of these pixels is reset by the proposed algorithm (Eq. (6)). The key to using the sawtooth pattern for wrapped phase conversion is the identification of local maximum (peak) and minimum (valley) intensities so that the translating parameters α and β associated with each cycle can be obtained. This is relatively easy since after intermediate pixels removal, a pair of peak and valley always appear to be adjacent to each other, as shown in Fig. 6(b). The program labels a local maximum as a

peak only if it is accompanied by a local minimum. A similar procedure applies to the identification of a valley. This approach is helpful for the reliability of the algorithm. Otherwise, if peaks and valleys are located only based on local extremes, numerous errors would be encountered because of the many local extremes in shadow areas hardly observable to the naked eye.

When local maxima (peaks) and minima (valleys) are located, the translating parameters associated with each cycle are obtained. The intensities of each cycle are then converted to phase angles resulting in a wrapped phase map, as shown in Fig. 4. Fig. 6(c) shows the phase distribution of cross-section *A–A* after conversion. It is seen that uniform values of peaks and valleys are obtained; while before conversion (Fig. 6(b)), the peaks and valleys are non-uniform.

4.2. Comparison of quality maps

To unwrap the phase map shown in Fig. 4, a quality-guided phase unwrapping algorithm is used. This is guided by a phase derivative variance map [17,18] and the proposed plane-fitting map. The quality-guided phase unwrapping is an integration process, in which the unwrapped phase value of a pixel is dependent on the phase values of pixels that have been unwrapped. Low quality shadow areas at the edge, fin and tail of the fish model should be unwrapped at a later stage so that unwrapping errors can be confined to a minimum area. However, if shadow areas are erroneously labeled as high quality and unwrapped at an early stage, unwrapping errors would begin to accumulate and affect all subsequent results.

The phase derivative variance map is sensitive to noise. The higher the noise, the larger is the variance and hence low quality. However, the variance map shown in Fig. 7(a) is not able to detect the low quality data at the fin and tail of the fish model because shadow turns out to be smooth phase data. Furthermore, although it identifies some low quality data at the edge of the fish model, the low quality regions are disconnected, making it possible for the unwrapping path to move in and out of the fish body from the gaps, which would cause errors. The unwrapped result guided by the variance map is shown in Fig. 7(b). There is a large discontinuous area at the top left corner of the background. Intuitively, the error must have come from the edge of the fish model and penetrated into the background. It is note worthy that the variance map would have better performance if the phase-shifting algorithm is used to extract the wrapped phase map, since shadow would become drastically changing noisy data after being processed by the phase-shifting algorithm.

The present proposed quality criterion evaluates the fitted plane of a $N \times N (N = 5)$ neighborhood of a pixel under consideration. The quality is related to the normal vector of the plane and the fitting error. Fig. 8(a) shows the plane-fitting quality map. Phase data on the edge, fin and tail of the fish model are all labeled as low quality. It also shows periodically changing quality stripes on the background and the fish model body but where uniform quality distribution is supposed to be found. These stripes are caused by the system nonlinearity. Although the data plane of a computer-generated sawtooth pattern has an identical normal vector, the plane is slightly curved when the sawtooth pattern is

projected and imaged, which can be seen in Fig. 5(a). The curvature of each cycle is similar resulting in a periodically changing k_x of the normal vector of the fitted plane. Therefore, a periodically changing quality stripes are formed. However, since even the low quality stripes have higher values than those of shadow areas, they would be unwrapped earlier. Consequently, the unwrapping errors are confined to shadow areas, as shown in Fig. 8(b).

4.3. Accuracy

The results of one-frame sawtooth pattern projection technique are compared with phase-shifting technique [11] using results obtained from a contact profilometer. Fig. 9(a) shows the height of cross-section *B–B*, as indicated in Fig. 8(b), obtained by the proposed method and the contact profilometer. As can be seen, the results do not agree well near the fish model mouth and fin, where shadow has distorted the recorded intensity and subsequently reduced the reliability and quality of the data. Fig. 9(b) shows a comparison between the phase-shifting technique and the contact profilometer for the same cross-section. Since phase shifting is less dependent on intensity, it successfully retrieves the profile at the mouth area. However, at the fin area as large shadow has completely removed the fringe signals, even the phase-shifting technique could not recover the actual profile. At the fish model main body, the accuracy of phase shifting is also higher than the proposed method which gives a profile containing unappreciable ripples (Fig. 9(a)).

Several factors such as system nonlinearity, non-uniform reflectance, and random noise could affect the accuracy of the present method. The major source of error comes from system nonlinearity. Though linear intensity range is used to generate the sawtooth pattern, as described in Section 3, nonlinearity related errors are still significant as shown by the ripples in Fig. 9(a). This should be the basis for future research. Non-uniform reflectance is another source of error. Since intensity and phase value are coupled as shown in Eq. (7), any change in reflectance would introduce a phase change. Although the translation from intensity to phase is performed locally to enhance the tolerance to non-uniform reflectance, the method is more dependent on the modulation intensity than the phase-shifting algorithm and therefore the latter gives better results at the fish model mouth. Random noise, such as exceptionally high or low intensity pixels, is not frequently encountered in this study. Nevertheless, if encountered, it would bring errors into the identification of peak and valley intensities. With proper arrangement of the experimental set-up and by using high quality projection and imaging devices, random noise can be minimized.

5. Concluding remarks

Unlike conventional sinusoidal or square wave fringe pattern shape-encoding method, the proposed technique is based on the inherent sawtooth characteristics both in a sawtooth pattern and in a wrapped phase map. The algorithm extracts wrapped phase data from recorded intensity pattern by means of a linear translation. Hence, multiple

recording of phase-shifted images or image of specific sizes for fast Fourier transform (FFT) process is not necessary. Linear translation of intensity to phase angle is carried out locally to reduce system nonlinearity effect and the accuracy of the method increases with the uniformity of an object surface reflectance. A phase quality criterion based on the least-square plane-fitting is also proposed to minimize shadow related errors in the phase unwrapping process. Using the proposed quality map, a correct phase distribution is retrieved and phase unwrapping errors are confined to shadow areas.

References

[1] F. Chen, G.M. Brown, M. Song, Opt. Eng. 39 (2000) 10.

[2] H. Takasaki, Appl. Opt. 9 (1970) 1467.

[3] D.M. Meadows, W.O. Johnson, J.B. Allen, Appl Opt. 9 (1970) 942.

[4] D. Malacara, Optical Shop Testing, second ed., Wiley, New York, 1992.

[5] H.J. Tiziani, Proc. SPIE 381 (1983) 209.

[6] J.W. Wyant, Laser Focus 381 (May) (1982) 65.

[7] G.G. Kino, S.S.C. Chim, Appl. Opt. 29 (1990) 3775.

[8] J.C. Wyant, Proc. SPIE 4737 (2002) 98.

[9] X.Y. Su, W.S. Zhou, G. von Bally, D. Vukicevic, Opt. Commun. 94 (1992) 561.

[10] M. Takeda, K. Mutoh, Appl. Opt. 22 (1983) 3977.

[11] V. Srinivasan, H.C. Liu, M. Halioua, Appl. Opt. 23 (1984) 3105.

[12] C.R. Coggrave, J.M. Huntley, Opt. Eng. 39 (2000) 91.

[13] G. Sansoni, S. Corini, S. Lazzari, R. Rodella, F. Docchio, Appl. Opt. 36 (1997) 4463.

[14] C. Quan, X.Y. He, C.F. Wang, C.J. Tay, H.M. Shang, Opt. Commun. 189 (2001) 21.

[15] P.S. Huang, Q. Hu, F. Jin, F.P. Chiang, Opt. Eng. 38 (1999) 1065.

[16] Q. Fang, S. Zheng, Appl. Opt. 36 (1997) 2401.

[17] D.C. Ghiglia, M.D. Pritt, Two-Dimensional Phase Unwrapping, Wiley, New York, 1998.

[18] M.D. Pritt, IEEE Trans. Geosci. Remote Sensing 34 (3) (1996) 728.

[19] C. Quan, C.J. Tay, L. Chen, Y. Fu, Appl. Opt. 42 (2003) 7060.

List of Figures

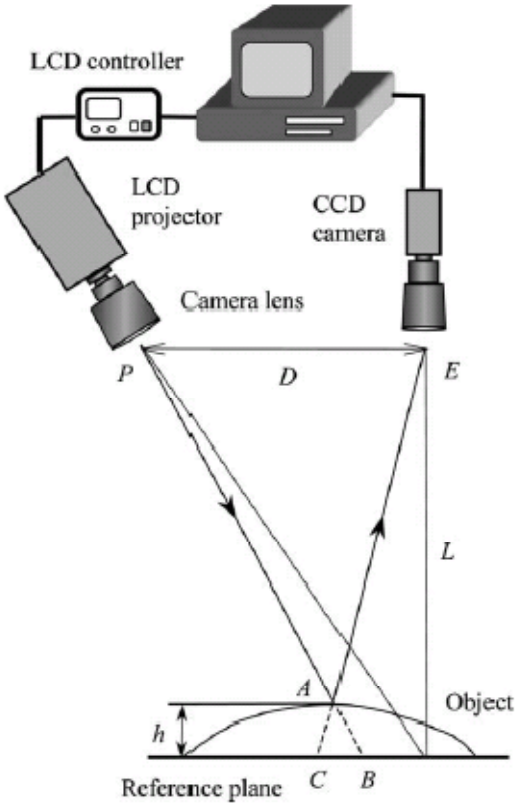
LCD controller
LCD
projector
CCD
camera
Camera lens
P
D
E
L
A
Object
h
Reference plane
C
B

Fig. 1

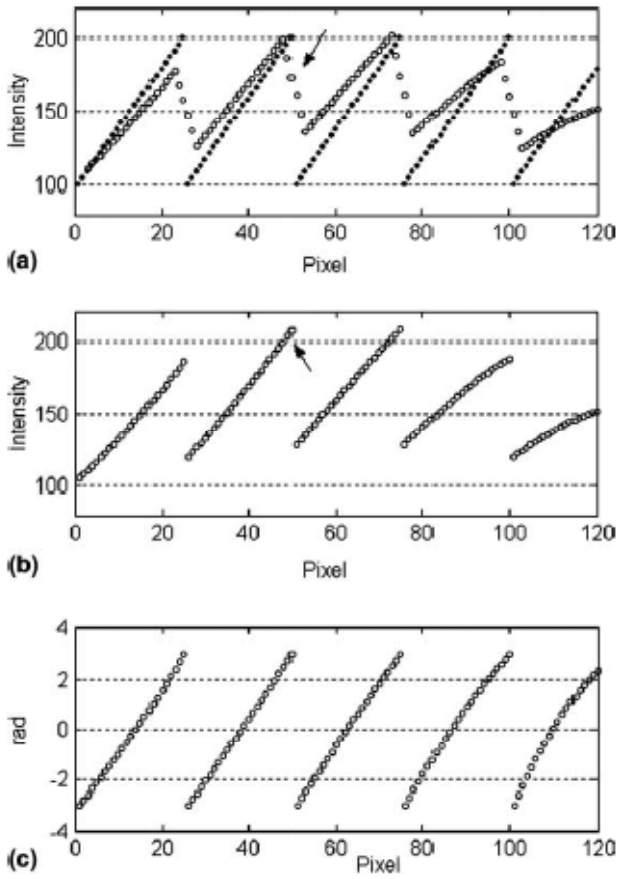
Intensity
200
150
100
0
20
40
60
80
100
120
Pixel
(a)
Intensity
200
150
100
0
20
40
60
80
100
120
Pixel
(b)
rad
4
2
0
-2
-4
0
20
40
60
80
100
120
Pixel
(c)

Fig. 2

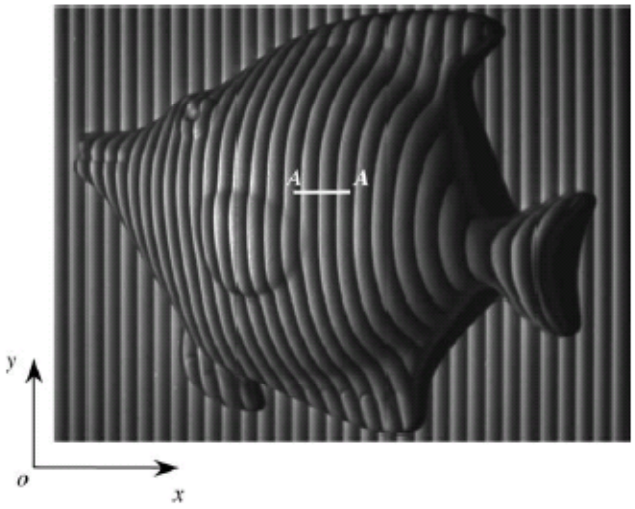

Fig. 3

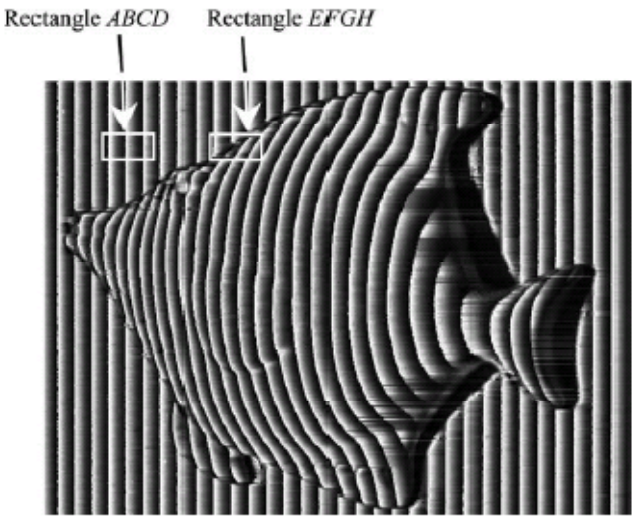

Fig. 4

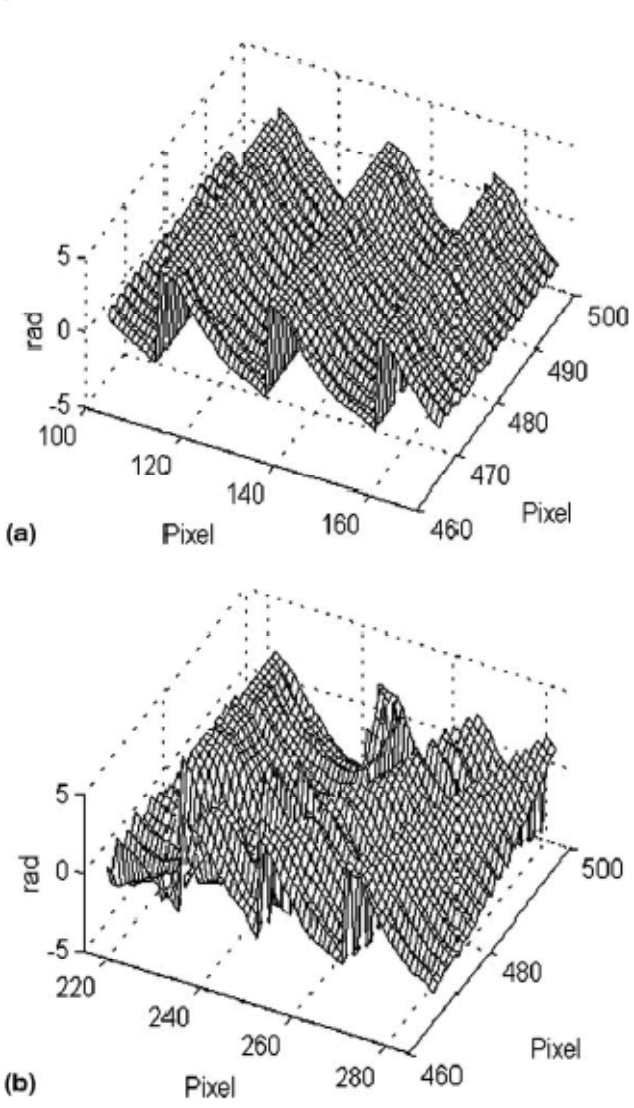
5
0
-5
rad
100
120
140
160
Pixel
(a)
460
470
480
490
500
Pixel
5
0
-5
rad
220
240
260
280
Pixel
(b)
460
480
500
Pixel

Fig. 5

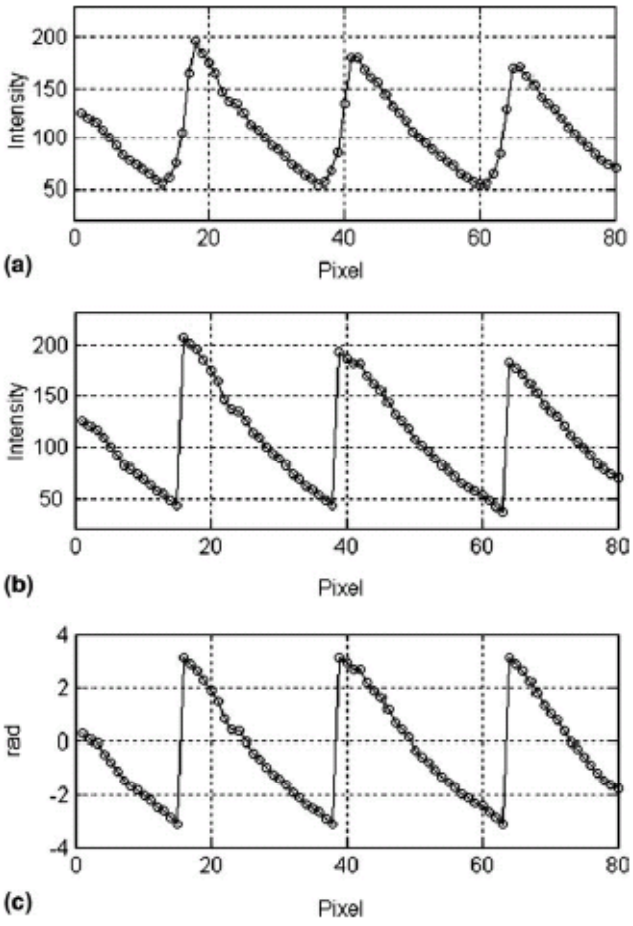
Intensity
200
150
100
50
0
20
40
60
80
Pixel
(a)
Intensity
200
150
100
50
0
20
40
60
80
Pixel
(b)
rad
4
2
0
-2
-4
0
20
40
60
80
Pixel
(c)

Fig. 6

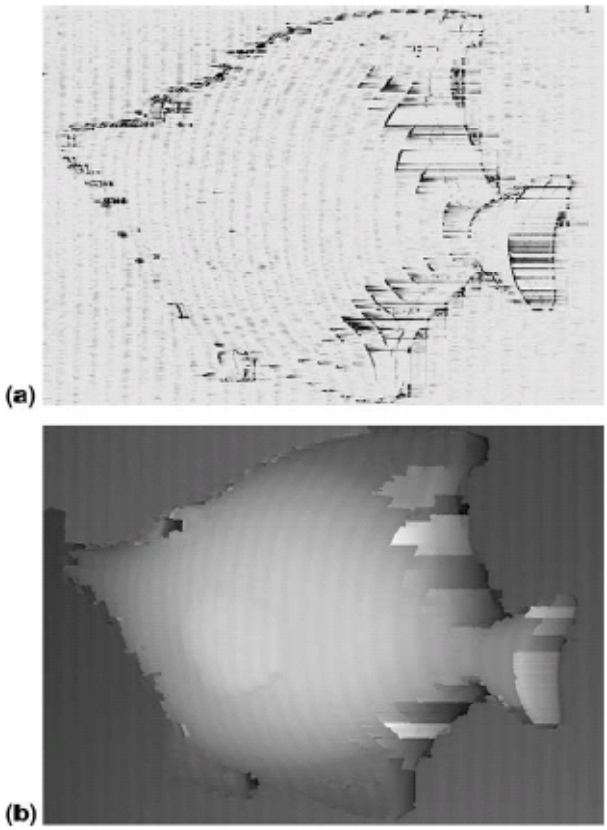

Fig. 7

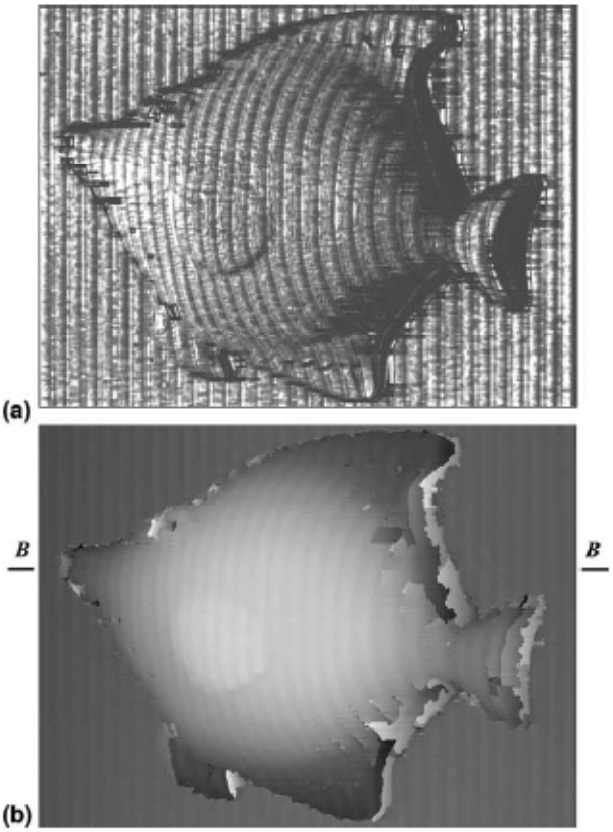

Fig. 8

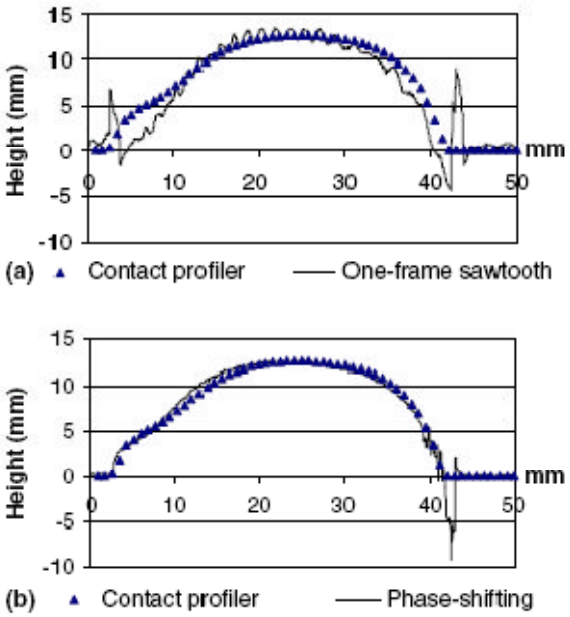
15
10
5
0
-5
-10
Height (mm)
0
10
20
30
40
50
mm
(a)
Contact profiler
One-frame sawtooth
15
10
5
0
-5
-10
Height (mm)
0
10
20
30
40
50
mm
(b)
Contact profiler
Phase-shifting

Fig. 9